

Electronic Supplementary Information (ESI):

This journal is © The Royal Society of Chemistry 2022

(Et₄N)[W^{III}(DAPBH)(CN)₂], the first pentagonal-bipyramidal W(III) complex with unquenched orbital angular momentum: a novel Ising-type magnetic building block for single-molecule magnets

Yu. V. Manakin,^{*a} V. S. Mironov,^{*a,b} T. A. Bazhenova,^a I. A. Yakushev,^{c,d} I. F. Gilmudinov,^e S. V. Simonov^f and E. B. Yagubskii^{a*}

^a Federal Research Center of Problems of Chemical Physics and Medicinal Chemistry RAS, Chernogolovka, Russia, E-mail: george@icp.ac.ru; yagubski@icp.ac.ru.

^b Shubnikov Institute of Crystallography of Federal Scientific Research Centre “Crystallography and Photonics” RAS, Moscow, Russia. E-mail: mirsa@list.ru.

^c Kurnakov Institute of General and Inorganic Chemistry, Moscow.

^d National Research Center “Kurchatov Institute”, Moscow, Russia

^e Institute of Physics, Kazan Federal University, Kazan, Russia

^f Institute of Solid State Physics, Chernogolovka, Russia

1. PHYSICAL MEASUREMENTS

IR spectra were recorded with a Perkin Elmer SPECTRUM TWO FT-IR spectrometer in the range of 4000–600 cm⁻¹. Elemental analyses were performed by the Analytical Department service at the Institute of Problems of Chemical Physics using a Vario MICRO Cube analyzer. ¹H NMR spectra were recorded on a Bruker Avance III 500 MHz NMR spectrometer at the Multi-User Analytical Center of Federal Research Center of Problem of Chemical Physics and Medicinal Chemistry RAS. Magnetic measurements were performed using vibrating-sample magnetometer (VSM) installed to physical properties measurements system (PPMS-9, Quantum Design) and have been supported by the Kazan Federal University Strategic Academic Leadership Program (PRIORITY-2030). Polycrystalline samples were loaded into gelatin capsules and glued to a standard copper holder. The experimental data were corrected for the sample holder and the capsule. The diamagnetic contribution was calculated using Pascal’s constants.

2. MATERIALS AND METHODS

All operations, except where otherwise stated, were carried out under argon atmosphere. W(CO)₆ (Acros), Ag(CF₃SO₃) (Aldrich), Mn(ClO₄)₂ (hydrate, Aldrich), Et₄NCl (Aldrich), N,N-dimethylformamide (ABCR) were used as received. Ferrocene and iodine were purified by double sublimation. Sodium cyanide was dried at 150°C under dynamic vacuum for several hours.

Acetonitrile, methylene chloride and pyridine were distilled over calcium hydride. Diethyl ether and tetrahydrofuran were distilled over LiAlH₄. All the solvents were purged with argon and stored over molecular sieves 3 Å prior to use. Wl₂(CO)₃(MeCN)₂, [Cp₂Fe](OTf) and H₂DAPBH were prepared according to the reported methods [S1,S2,S3].

[W^{II}(DAPBH)(CO)Py] (4)

3 ml of pyridine were added to the mixture of 199 mg (0.33 mmol, slight excess) of Wl₂(CO)₃(MeCN)₂ and 130 mg (0.32 mmol) of H₂DAPBH. The mixture was stirred under reduced pressure at 40°C for 2 hours, until dissolution of solids was complete. Cooled solution was then filtered and layered with 15 ml of acetonitrile. After diffusion has completed (1 week), black lustrous crystals of the product (140 mg) were collected, rinsed with acetonitrile and dried under vacuum. The filtrate was concentrated to almost dryness and diluted with 15 ml of acetonitrile to give another crop of the product. The combined yield was 70-80%. FT-IR (cm⁻¹): 619 w; 651 m; 694 vs; 715 m; 757 s; 767 s; 788 m; 838 w; 901 m; 923 w; 985 s; 1003 s; 1026 w; 1067 m; 1090 w; 1137 s; 1156 m; 1173 s; 1218 w; 1270 s; 1303 m; 1339 vs; 1365 vs; 1406 s; 1444 s; 1485 s; 1517s; 1583 w; 1819 vs (coordinated CO); 3057 w; 3624 w. ¹H NMR (d₅-Pyridine, 500 MHz): δ = 8.62 (2H, d, *J* = 5.2 Hz), 8.55 (4H, d, *J* = 7.5 Hz), 7.44 (6H, m), 7.34 (1H,t, *J* = 7.5 Hz), 7.08 (2H, t, *J* = 6.8 Hz), 6.71 (2H, d, *J* = 7.8 Hz), 6.22 (1H, t, *J* = 7.8 Hz), 2.92 (6H, s) ppm. Found: C, 50.89; H, 3.51; N 12.31%. Calc. for C₂₉H₂₄N₆O₃W: C, 50.60; H, 3.51; N, 12.21%.

Solid **4** is quite stable to oxygen and moisture and can be weighed in air. Solutions of **4** in chlorinated solvents (methylene chloride, chloroform) quickly decompose.

(Et₄N)[W^{III}(DAPBH)(CN)₂] (6)

7 ml of DMF were added to freshly dried NaCN (63 mg; 1.285 mmol) and **4** (440 mg; 0.64 mmol). The mixture was stirred under reduced pressure at 70°C for 10 hours, as the color changed from brownish purple to dark yellow. The liquids were removed *in vacuo* affording dark yellow extremely air sensitive polycrystalline material (**5'**). To this was added two equivalents of Et₄NCl in 20 ml of acetonitrile. After 10 hours of stirring, one equivalent of [Cp₂Fe](OTf) (214 mg) in 20 ml of acetonitrile was added dropwise. The resulting dark emerald green solution was filtered from NaCl and dried under vacuum. The solid was dissolved in 4 ml of DMF and layered with 15 ml of THF. Black crystals of the product (265 mg) were collected after 2 weeks, washed thoroughly with THF, ether and dried under vacuum. The yield was 50-60%. FT-IR (cm⁻¹): 638m; 670 s; 704 vs; 783 s; 814 s; 881 m; 933 m; 1000 m; 1030 m; 1070 m; 1140 m; 1171 s; 1263 s; 1333 m; 1366 s; 1392 s; 1447 s; 1484 s; 1517 m; 2106 w; 2987 w; 3061 w. Found: C, 52.00; H, 5.06; N 14.02; S, 0.00 %. Calc. for C₃₃H₃₉N₈O₂W: C, 51.91; H, 5.15.; N, 14.68 %.

Widely used $[\text{Cp}_2\text{Fe}]\text{PF}_6$ worked as well in the above preparation but led to severe contamination of **6** (probably by $(\text{Et}_4\text{N})\text{PF}_6$). Complex **6** is highly sensitive to air and light.



Hydrate of $\text{Mn}(\text{ClO}_4)_2$ was dissolved in DMF and dried under vacuum. This was repeated twice after which the residue was re-dissolved in DMF and added to the equimolar solution of **6** in DMF. The solution was layered with excess of diethyl ether and left for crystallization for several weeks. Black crystalline material was collected on a filter, washed with ether and quickly dried under vacuum. The product was impure, so magnetic properties were not investigated.

3. X-RAY CRYSTALLOGRAPHY

X-ray structure determination of **4**, **6**, **7**

X-ray diffraction data for **4** was collected on the “Belok” beamline at the Kurchatov Synchrotron Radiation Source (National Research Center “Kurchatov Institute”, Moscow, Russian Federation) in φ -scan mode using SX165 CCD detector (Rayonix, Evanston, IL, USA), $\lambda = 74503 \text{ \AA}$ [S4]. The X-ray diffraction for the complexes **6** and **7** were obtained on a Bruker D8 Venture Photon single crystal diffractometer equipped with microfocus sealed tube Incoatec $\text{I}\mu\text{S}$ 3.0 (Mo $K\alpha$ radiation, $\lambda = 0.71073 \text{ \AA}$) in φ - and ω -scan mode at the Center of shared equipment IGIC RAS. The raw reflection intensities for **4** was indexed, integrated and scaled with the *XDS* data reduction program [S5]; the raw data for **6** and **7** were treated with the *APEX3* program suite [S6]. Experimental intensities were corrected for absorption effects using *SADABS* [S6] and *TWINABS* programs [S7] for **6** and **7**, respectively. The crystal structures were solved by direct methods [S8] and refined by the full-matrix least-squares on F^2 [S9] using *OLEX2* structural data analysis program suite [S10]. All non-hydrogen atoms were refined applying anisotropic displacement parameters without any constraints or restraints for **4**, **6**, **7**, and the hydrogen atoms were placed in the ideal calculated positions and refined isotropically using the riding model with $U_{\text{iso}}(\text{H}) = 1.5U_{\text{eq}}(\text{C})$ for the methyl groups and with $U_{\text{iso}}(\text{H}) = 1.2U_{\text{eq}}(\text{C})$ for other hydrogen atoms

Table S1. Crystal data and structure refinement parameters for **4**, **6**, **7**.

Sample	4	6	7
CCDC	2161096	2161097	2217467
Brutto formula	$\text{C}_{29}\text{H}_{24}\text{N}_6\text{O}_3\text{W}$	$\text{C}_{37}\text{H}_{39}\text{N}_8\text{O}_2\text{W}$	$\text{C}_{40}\text{H}_{54}\text{MnN}_{12}\text{O}_{11}\text{WCl}$
Formula weight	688.39	811.60	1153.16
T, K	100	100	150
Space group	$\text{P2}_1/\text{n}$	$\text{Pna}2_1$	$\text{P2}_1/\text{c}$

Z(Z')	4(1)	4(1)	4(1)
a/Å	7.9393(16)	22.4973(6)	17.5299(12)
b/Å	21.1967(12)	10.7901(3)	14.7868(10)
c/Å	14.8915(11)	13.0307(3)	18.6121(12)
α /°	90	90	90
β /°	92.545(5)	90	93.389(2)
γ /°	90	90	90
Volume/Å ³	2503.57	3163.18(14)	4816.0(6)
ρ_{calc} , g/cm ³	1.826	1.603	1.590
μ /cm ⁻¹	5.221	3.696	2.773
F(000)	1352	1532	2328
2 θ_{max} , °	57	57.2	55.4
Reflections collected (R _{int})	54069 (0.0412)	48678 (0.0383)	8487 (0.0917)
Independent reflections	5475	8125	8487
Reflections with I>2 σ (I)	5002	6961	7009
R ₁ [I>2 σ (I)]	0.0230	0.0293	0.0479
wR ₂	0.0621	0.0639	0.1342
GOF	1.019	1.061	1.050
Residual electron density, e·Å ⁻³ ($\rho_{\text{min}}/\rho_{\text{max}}$)	-0.913/1.450	-1.148/1.602	-1.151/2.547

Table S2. Selected bond lengths (Å) and angles (°) in **4**, **6**, **7***.

Bonds	4	Bonds	6	Bonds	7
W1-N1(pyridine)	2.263	W1-C1(cyanide)	2.169	W1-C31(cyanide)	2.152
W1-C29(carbonyl)	1.946	W1-C2(cyanide)	2.169	W1-C41(cyanide)	2.161
W1-N4	2.103	W1-N5	2.044	W1-N3	2.060
W1-N3	2.116	W1-N4	2.088	W1-N2	2.069
W1-N5	2.119	W1-N6	2.083	W1-N4	2.087
W1-O2	2.113	W1-O1	2.073	W1-O1	2.067
W1-O3	2.103	W1-O2	2.067	W1-O2	2.076
Angles		Angles		Angles	
N1-W1-C29	176.72	C1-W1-C2	171.51	C31-W1-C41	169.30
O2-W1-N3	71.76	O1-W1-N4	71.47	O1-W1-N2	72.30
N3-W1-N4	70.71	N4-W1-N5	71.25	N2-W1-N3	70.89

N4-W1-N5	70.94	N5-W1-N6	71.84	N3-W1-N4	70.87
N5-W1-O3	71.55	N6-W1-O2	70.95	N4-W1-O2	71.50
O2-W1-O3	74.64	O1-W1-O2	74.80	O1-W1-O2	74.54

Fig. S1. X-ray crystal structure of **7**. A fragment of chain is depicted. Hydrogen atoms were omitted for clarity.

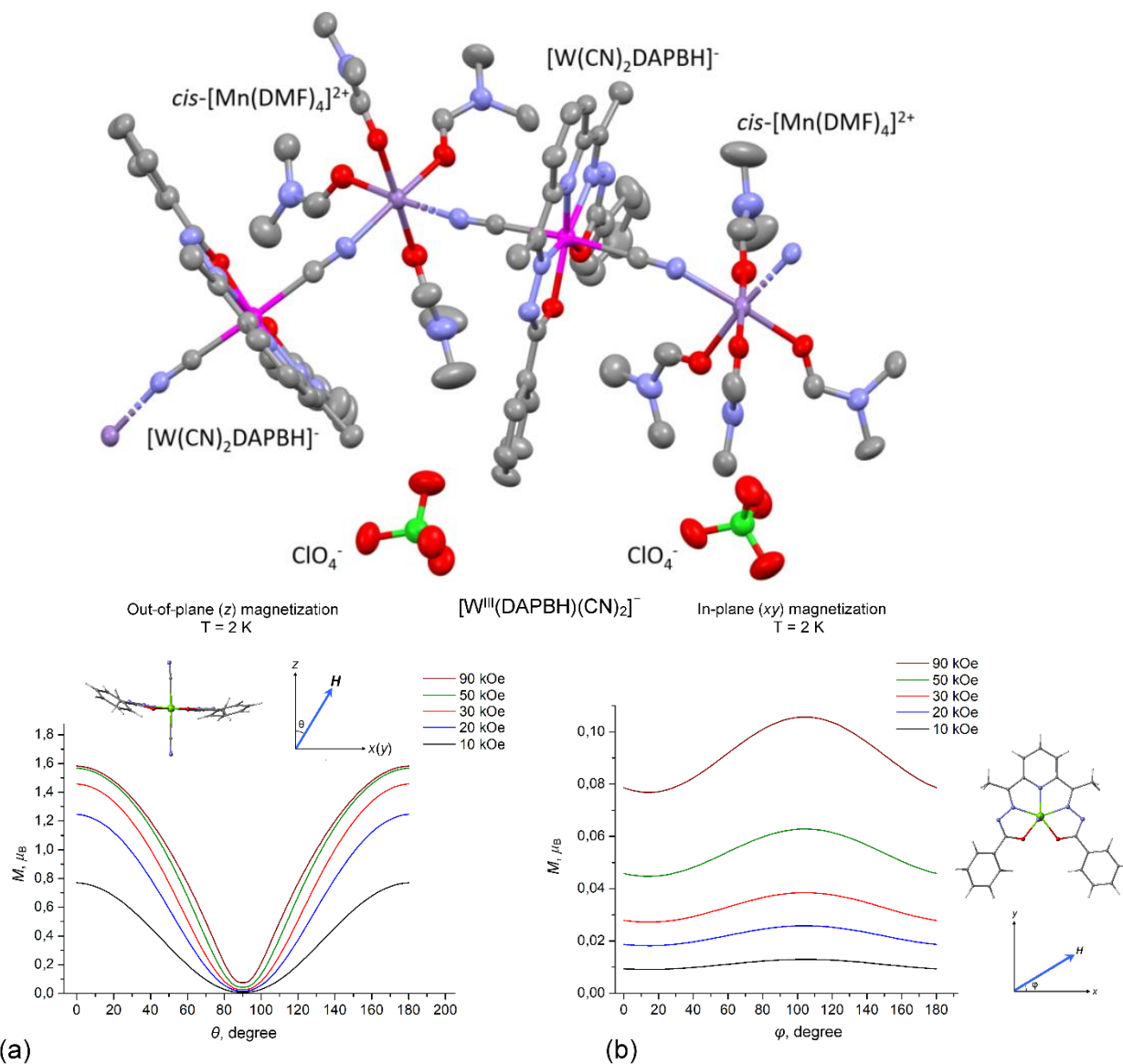


Fig. S2. Calculated angular variation of the magnetization $M(\theta, \phi, H)$ of single crystals of $(\text{Et}_4\text{N})[\text{W}^{\text{III}}(\text{DAPBH})(\text{CN})_2]$, (a) out-of-plane magnetization $M(\theta)$ vs. θ at $T = 2 \text{ K}$ and variable magnetic field. The magnetization $M(\theta)$ reveals very strong easy-axis anisotropy, $M(\theta = 0^\circ) \gg M(\theta = 90^\circ)$; in a strong magnetic field, the easy-axis magnetization $M(\theta = 0^\circ)$ saturates at $\sim 1.6 \mu_B$, while the in-plane magnetization $M(\theta = 90^\circ)$ remains very low ($< 0.1 \mu_B$), even at $H = 90 \text{ kOe}$; (b) in-plane magnetization $M(\phi)$ vs. ϕ (at $\theta = 90^\circ$, $H \parallel xy$) at $T = 2 \text{ K}$. The dependence of the in-plane magnetization $M(\phi)$ on the azimuthal angle ϕ is much less pronounced, thus indicating a nearly perfect uniaxial symmetry of magnetic anisotropy (of the Ising-type) of the $[\text{W}^{\text{III}}(\text{DAPBH})(\text{CN})_2]^-$ complex. In fact, the in-plane magnetization $M(\theta = 90^\circ, \phi, H)$ increases linearly with the increasing field H , i.e., $M(\theta = 90^\circ, \phi, H) \approx (H/H_0)M(\theta = 90^\circ, \phi, H_0)$ thereby resulting in temperature-independent paramagnetism.

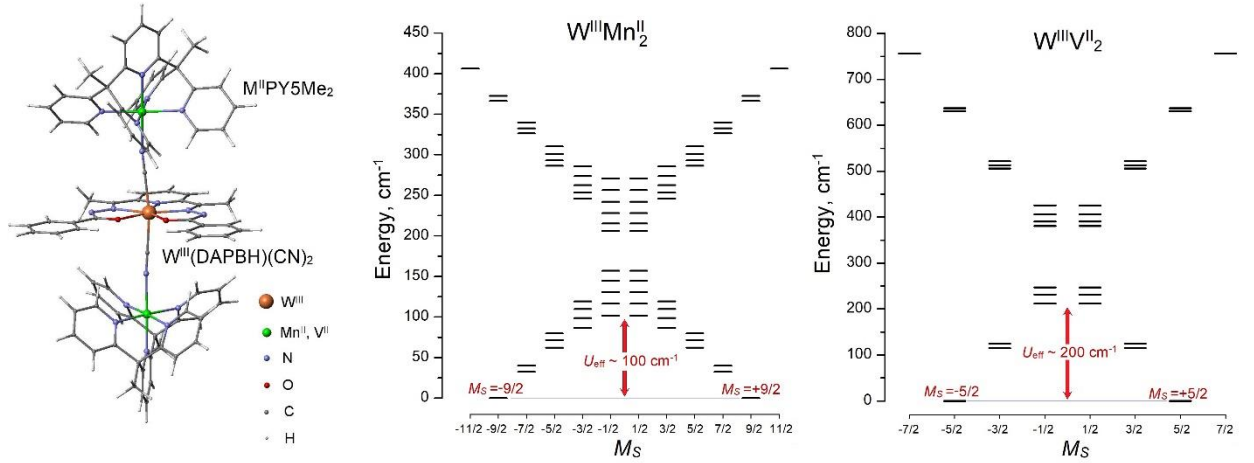


Fig. S3. The supposed structure of the trinuclear cyano-bridged clusters $M^{\text{II}}\text{-NC-W}^{\text{III}}\text{-CN-M}^{\text{II}}$ (where $M^{\text{II}} = \text{Mn}^{\text{II}}, \text{V}^{\text{II}}$) composed of the central PBP complex $[\text{W}^{\text{III}}(\text{DAPBH})(\text{CN})_2]^-$ and two high-spin 3d ions ($\text{Mn}^{\text{II}}, \text{V}^{\text{II}}$) encapsulated into pentadentate ligand PY5Me_2 . These clusters are analogs of the $\text{Mo}^{\text{III}}\text{Mn}^{\text{II}}_2$ SMM clusters with the central PBP complex $[\text{Mo}^{\text{III}}(\text{CN})_7]^{4-}$ reported in ref. ¹³ in the main text. The expected double-well energy profile of the spin energy levels and estimated energy barrier U_{eff} ($\sim 100 \text{ cm}^{-1}$ for WMn_2 and $\sim 200 \text{ cm}^{-1}$ for WV_2) are shown. The spin energy diagrams E vs. M_S are calculated with estimated anisotropic exchange parameters $J_z = -80, J_{xy} = -30 \text{ cm}^{-1}$ for WMn_2 and $J_z = -250, J_{xy} = -50 \text{ cm}^{-1}$ for WV_2 .

4. THEORETICAL CALCULATIONS

4.1. Ligand-field (LF) and angular-overlap model (AOM) calculations and simulation of magnetic susceptibility and magnetization

Ligand-field (LF) calculations for the $[\text{W}^{\text{III}}(\text{DAPBH})(\text{CN})_2]^-$ complex are performed in terms of a model Hamiltonian

$$H = \sum_{i>j} \frac{e^2}{|\mathbf{r}_i - \mathbf{r}_j|} + \zeta_W \sum_i \mathbf{L}_i \mathbf{S}_i + V_{\text{LF}} + \mu_B (k\mathbf{L} + 2\mathbf{S})\mathbf{H}, \quad (\text{S1})$$

in which the first term represents Coulomb repulsion between 5d electron of W^{III} (where i and j numerate 5d electrons), the second term is the spin-orbit coupling (SOC) of W^{III} , V_{LF} is a ligand-field Hamiltonian, and the last term represents the Zeeman interaction with the external magnetic field \mathbf{H} . In these calculations, the $B = 400$ and $C = 2000 \text{ cm}^{-1}$ Racah parameters for the Coulomb term in (S1), the SOC constant $\zeta_W = 1800 \text{ cm}^{-1}$, and the $k = 0.62$ orbital reduction factor in the Zeeman term were applied. The one-electron operator V_{LF} is calculated in terms of the angular overlap model (AOM). [S11] For N and O atoms in the N_3O_2 chelate ring we used the AOM parameters $e_\sigma = 15000 \text{ cm}^{-1}$ and $e_\pi/e_\sigma = 0.25$, which approximately correspond to a typical $10Dq \approx 30000 \text{ cm}^{-1}$ crystal-field splitting energy of 5d metal ions with moderately strong ligands from the spectrochemical series, as can be estimated from the Jorgensen's equation [S12]; AOM parameters for the apical CN groups are set to $e_\sigma = 20000 \text{ cm}^{-1}$ and $e_\pi/e_\sigma = 0.25$. The radial dependence of the AOM parameters for N and O atoms in the N_3O_2 pentagon was approximated by $e_{\pi,\sigma}(R) = e_{\pi,\sigma}(R_0)(R_0/R)^n$ with $n = 3$ at the reference distance $R_0 = 2.10 \text{ \AA}$. Energy levels of the $5d^3$ LF states of W^{III} are obtained by a numerical diagonalization of (S1) in the full set of $5d^3$ wave

functions involving 120 $|LM_LSM_S\rangle$ microstates. The actual experimental geometry of $[\text{W}^{\text{III}}(\text{DAPBH})(\text{CN})_2]^-$ complex was applied.

The components M_α ($\alpha = x, y, z$) of the magnetic moment \mathbf{M} of $[\text{W}^{\text{III}}(\text{DAPBH})(\text{CN})_2]^-$ in an external magnetic field \mathbf{H} are obtained from the conventional equation

$$M_\alpha = Nk_B T \frac{\partial \ln Z(H)}{\partial H_\alpha}, \quad (\text{S2})$$

where $Z(\mathbf{H})$ is the partition function

$$Z(\mathbf{H}) = \sum_i \exp\left(-\frac{E_i(\mathbf{H})}{k_B T}\right), \quad (\text{S3})$$

with $E_i(\mathbf{H})$ being the energy of the i -th electronic state of the W^{III} ion in the magnetic field \mathbf{H} obtained from diagonalization of the spin Hamiltonian (S1). Then the diagonal component $\chi_{\alpha\alpha}$ of the tensor of magnetic susceptibility is written as $\chi_{\alpha\alpha} = M_\alpha/H_\alpha$; magnetic susceptibility of the powder sample is given by $\chi = (\chi_{xx} + \chi_{yy} + \chi_{zz})/3$. Calculations for **6** are performed at the experimental applied field of $H = 5 \text{ kOe}$.

The field dependence of magnetization $\mathbf{M}(\mathbf{H})$ for powder samples is calculated in two steps. First, the magnetization \mathbf{M} is calculated as a function of the spherical angles θ, φ and applied magnetic field \mathbf{H} , $\mathbf{M} = \mathbf{M}(\theta, \varphi, H)$, and then the average $M(H)$ dependence for a powder sample is obtained by integration over the whole (θ, φ) sphere referring to the random angular orientation of microcrystals,

$$M(H) = \frac{1}{4\pi} \int_0^{2\pi} d\varphi \int_0^\pi M(\theta, \varphi, H) \sin\theta d\theta, \quad (\text{S4})$$

where the polar angle θ corresponds to the angle between the pentagonal axis of $[\text{W}^{\text{III}}(\text{DAPBH})(\text{CN})_2]^-$ complex and the applied magnetic field H and φ is the azimuthal angle in the equatorial plane N_3O_2 (Fig. S2).

Calculated energies of 5d orbitals, 5d³ LF states, and spin-orbit 5d³ states of $[\text{W}^{\text{III}}(\text{DAPBH})(\text{CN})_2]^-$ are presented, respectively, in Tables S3, S4, and S5.

Table S3. Calculated LF splitting energies (cm^{-1}) of 5d orbitals in the $[\text{W}^{\text{III}}(\text{DAPBH})(\text{CN})_2]^-$ complex.

5d orbital	E
$5d_{xz}$	0
$5d_{yz}$	315
$5d_{x^2-y^2}$	21946
$5d_{xy}$	23110
$5d_{z^2}$	29725

Table S4. Calculated energies (cm^{-1}) of LF states ($5d^3$) of $[\text{W}^{\text{III}}(\text{DAPBH})(\text{CN})_2]^-$ complex **6**. The two lowest energy levels (marked in red) correspond to the two orbital components ${}^2\Phi_{yz} = (xz)^2(yz)^1$ and ${}^2\Phi_{xz} = (yz)^2(xz)^1$ of the split orbital doublet ${}^2\Phi(M_L=\pm 1)$ (see Fig. 3 in the main text). Excited quartet spin states ($S=3/2$) are marked in blue.

Energy, cm^{-1}	${}^{2S+1}L$ atomic term composition, %			
	0	${}^2\text{H}$	33.35	${}^2\text{G}$
311	${}^2\text{H}$	33.45	${}^2\text{G}$	21.23
9817	${}^4\text{F}$	99.92	${}^4\text{P}$	0.08
10996	${}^4\text{F}$	99.72	${}^4\text{P}$	0.28
18533	${}^2\text{G}$	61.07	${}^2\text{H}$	31.90
18627	${}^2\text{G}$	57.60	${}^2\text{H}$	37.03
18818	${}^2\text{G}$	58.18	${}^2\text{D}$	26.73
19823	${}^2\text{G}$	58.21	${}^2\text{D}$	32.74
20086	${}^2\text{G}$	61.29	${}^2\text{D}$	6.39
20970	${}^2\text{P}$	43.67	${}^2\text{H}$	42.89
22218	${}^4\text{P}$	74.45	${}^4\text{F}$	25.55
24030	${}^2\text{H}$	25.55	${}^2\text{D}$	21.01
24822	${}^2\text{H}$	58.92	${}^2\text{D}$	27.85
29744	${}^2\text{H}$	44.21	${}^2\text{F}$	43.83
32895	${}^2\text{F}$	68.49	${}^2\text{D}(2)$	17.96
33116	${}^2\text{F}$	69.67	${}^2\text{D}(2)$	19.22
35072	${}^4\text{F}$	77.07	${}^4\text{P}$	22.93
35229	${}^4\text{F}$	77.49	${}^4\text{P}$	22.51
37822	${}^2\text{D}(2)$	63.06	${}^2\text{D}$	17.98
39823	${}^4\text{F}$	96.55	${}^4\text{P}$	3.45
39974	${}^4\text{F}$	98.06	${}^4\text{P}$	1.94

Table S5. Calculated energies (cm^{-1}) of low-lying $5d^3$ states of the $[\text{W}^{\text{III}}(\text{DAPBH})(\text{CN})_2]^-$ complex **6** with spin-orbit coupling $\zeta_w LS$ switched on (at $\zeta_w = 1800 \text{ cm}^{-1}$). The two lowest states correspond to the ground $\varphi(\pm 1/2)$ and excited $\chi(\pm 1/2)$ Kramers doublets of $[\text{W}^{\text{III}}(\text{DAPBH})(\text{CN})_2]^-$.

Energy, cm^{-1}
0
1711
9984
10337
11893
13418
18119
19458
19996
20913
21707
23014
23444

5. REFERENCES

- S1. P. K. Baker, S. G. Fraser and E. M. Keys, *J. Organomet. Chem.*, 1986, **309**, 319.
- S2. Y. Tanabe, K. Nakajima and Y. Nishibayashi, *Chem. Eur. J.*, 2018, **24**, 18618.
- S3. T. J. Giordano, G. J. Palenik, R. C. Palenik and D. A. Sullivan, *Inorg. Chem.*, 1979, **18**, 2445.
- S4. R. D. Svetogorov, P. V. Dorovatovskii and V. A. Lazarenko, *Cryst. Res. Technol.*, 2020, **55**, 1900184.
- S5. W. Kabsch, *Acta Crystallogr. D Biol. Crystallogr.*, 2010, **66**, 125.
- S6. APEX3, SAINT and SADABS. Bruker AXS Inc.: Madison, Wisconsin, USA, 2016.
- S7. G. M. Sheldrick. TWINABS, Ver. 2012/1. Madison, Wisconsin, USA: Bruker AXS, 2012.
- S8. G. M. Sheldrick, *Acta Cryst. A*, 2015, **71**, 3.
- S9. G. M. Sheldrick, *Acta Cryst. C*, 2015, **71**, 3.
- S10. O. V. Dolomanov, L. J. Bourhis, R. J. Gildea, J. A. K. Howard and H. Puschmann, *J. Appl. Cryst.*, 2009, **42**, 339.
- S11. (a) C. E. Schaeffer, C. K. Jorgensen, *Mol. Phys.*, 1965, **9**, 401; (b) C. E. Schaeffer, *Struct. Bonding*, 1968, **5**, 68.
- S12. C. K. Jorgensen, *Prog. Inorg. Chem.*, 1962, **4**, 73.